



Shale weathering profiles show Hg sequestration along a New York–Tennessee transect

Justin B. Richardson

Received: 16 April 2021 / Accepted: 22 September 2021
© The Author(s), under exclusive licence to Springer Nature B.V. 2021

Abstract Shale-derived soils have higher clay, organic matter, and secondary Fe oxide content than other bedrock types, all of which can sequester Hg. However, shales also can be Hg-rich due to their marine formation. The objectives of this study were to determine the concentration and phase partitioning of Hg in seven upland weathering profiles from New York to Tennessee USA and use geochemical normalization techniques to estimate the extent of Hg inheritance from weathering of shale bedrock or sequestration of atmospheric Hg. Total Hg concentrations in unweathered shale ranged from 3 to 94 ng/g. Total Hg concentrations decreased with depth in the Ultisols and Alfisols, with total Hg concentrations ranging from 18 to 265 ng/g. Across all shale soils and rocks, the oxidizable fraction of Hg (15% H₂O₂ extraction) comprised a large portion of the total Hg at 68% ± 8%. This fraction was dominated by organic matter as confirmed with positive correlations between Hg and %LOI, but could also be impacted by Hg sulfides. Across all sites, the reducible fraction of Hg (citrate-bicarbonate-dithionite extraction) was

only 10% ± 4% of the total Hg on average. Thus, secondary Fe oxides did not contain a significant portion of Hg, as commonly observed in tropical soils. Although colder sites had a higher organic matter and sequestered more Hg, τ values for Hg indexed to Ti suggest that atmospheric deposition, such as pollution sources in Ohio River Valley, drove the highest enrichment of Hg along the transect. These results demonstrate that shale-derived soils have a net accumulation and retention of atmospheric Hg, primarily through stabilization by organic matter.

Keywords Ultisols · Alfisols · Regolith · Mercury cycling · Critical zone

Introduction

Mercury is a toxic metal and global pollutant (Driscoll et al., 2013), which can negatively impact humans through chronic exposure, primarily through fish consumption (Holmes et al., 2009; Zahir et al., 2005). Understanding Hg sources and reservoirs is important for increasing sequestration of Hg from the atmosphere and limiting its movement into aquatic ecosystems where it can bioaccumulate (Amos et al., 2013; Lamborg et al., 2002). Despite its importance, Hg sequestration in the regolith (including soil, weathered bedrock, and bedrock) has been poorly

Supplementary Information The online version contains supplementary material available at <https://doi.org/10.1007/s10653-021-01110-x>.

J. B. Richardson (✉)
Department of Geoscience, University of Massachusetts
Amherst, 233 Morrill Science Center, Amherst,
MA 01003, USA
e-mail: jbrichardson@umass.edu

constrained. As demonstrated by Schuster et al., (2018) and Richardson et al., (2018), soils and weathered rock can act as a large Hg reservoir, which can potentially alter the local and regional Hg cycling by sequestering or releasing Hg to the atmosphere or river waters. In particular, shale weathering can release Hg to rivers with negative impacts on recreational fishing and fish consumption, which are popular activities throughout the Great Lake and Appalachian regions of the USA (Vaughan & Russell, 2015).

The sequestration of Hg in soil profiles and its relationship to bedrock are understudied. Most studies on the global Hg cycle focus on the top 0.3 m of the soil (e.g. Obrist et al., 2011; Richardson et al., 2013; Yu et al., 2014) because of the difficulty in physical excavation of samples due to strenuous work and necessity of specialized equipment and the assumption that most Hg cycling is sequestered within surface soils (the top 30 cm of soil). Because most soil pits are not deep enough to access the underlying lithology, their connection is often overlooked. In one of the few studies to examine diverse soil to bedrock relationships, Richardson et al., (2018) observed that Hg concentrations are very low in most crystalline igneous and metamorphic rocks are < 10 ng/g, but increased throughout the profile showing net accumulation and sequestration of Hg from the atmosphere. However, Richardson et al., (2018) also showed that sedimentary rocks can be Hg-rich and be a potential source for Hg to the critical zone. In studies conducted by Roulet et al., (1998) and Grimaldi et al., (2008), soils derived from quartz-kaolinite sedimentary rocks had soil Hg concentrations > 100 ng/g at depths below 2.0 m. Roulet et al., (1998) attributed the high soil Hg concentrations on the retention by Al and Fe oxides formed during pedogenesis. For this reason, younger, less developed soils may not sequester as much Hg as older, more developed soils. As soils undergo pedogenesis, they typically accumulate organic matter and precipitate Fe oxides, both of which are important for Hg adsorption and sequestration in temperate forested soils (Gabriel & Williamson, 2004; Richardson et al., 2013; Richardson et al., 2018; Schwesig & Matzner, 2001; Yu et al., 2014). Thus, it is essential to understand the role of both bedrock sourcing and pedogenesis on Hg sequestration to understand the role of soil as an Hg sink or source.

Shale is an important lithology both globally and for the USA due to its wide spatial abundance and its geochemistry (US EIA and Kuuskraa, 2011). Shale can have higher trace-element concentrations than igneous rocks like granite or metamorphosed rocks like schists. For example, Fu et al. (2015) showed that oil-bearing shales in China can have 28 to 13,890 ng/g Hg concentrations, which are far higher than typical granitoid rocks (see Adriano, 2001). In some systems, high geogenic Hg in shales and other sedimentary rocks can be inherited by the overlying soils. As a prime example, the soils derived from argillite *mélange* present at Eel River Critical Zone Observatory in California were substantially enriched in geogenic Hg (Tsui et al., 2014; Richardson et al., 2018). However, it can accumulate Hg as shales have high surface area due to their clay-sized fraction and diagenetic phyllosilicates, geogenic organic matter, and geogenic Fe oxides (Hosterman & Whitlow, 1981; Fu et al., 2015). Thus, soils derived from shale have multiple factors that can lead to their enrichment and sequestration of Hg. Lastly, Hg deposited to soils may be natural or anthropogenic. Grimaldi et al., (2008) estimated that atmospheric sources were responsible for up to 90% of the Hg sequestered by organic matter and oxides within a 3.0-m thick soil profile in French Guiana. Natural Hg emissions include volcanic activity and crustal degassing (Hylander & Meili, 2003; Nriagu & Becker, 2003). Natural Hg deposition occurs from fires, volcanoes, and gaseous Hg species in the air (Adriano, 2001; Streets et al., 2019). Anthropogenic Hg emissions include combustion of coal, industrial manufacturing, waste incineration, cement production, and mining activities (see Streets et al., 2017, 2019). Thus, it is essential to utilize geochemical tools, such as normalization to refractory indexing elements such as Ti and Zr, and to distinguish between added atmospheric Hg and shale inherited Hg. While this cannot distinguish between geogenic and anthropogenic Hg inputs, estimating sequestered from the atmosphere and inherited Hg from shale is key for determining whether the shale-derived soils are a net sink or source for local and regional watersheds.

The objectives of this study were to determine the concentration and phase of Hg in seven upland weathering profiles and use geochemical normalization techniques to estimate the extent of Hg inheritance from weathering of shale bedrock or from atmospheric inputs. Here, we leverage a climate

gradient transect from New York, USA south to Tennessee USA to examine the impact of soil development and varying to properties on Hg sequestration. It is anticipated that the either higher Hg in the shale bedrock could drive higher Hg in their overlying soils or the availability of organic matter and Fe oxides would promote Hg sequestration from atmospheric deposition. It is expected that warmer climates would have greater extent of pedogenesis to generate secondary Fe oxides (e.g., Grimaldi et al., 2008; Guedron et al., 2006; Richardson et al., 2018; Zhang et al., 2015), but cooler climates retain more organic matter for sorption (e.g., Obrist et al., 2011; Richardson et al., 2013; Yu et al., 2014). Next, it is hypothesized that soil Hg concentrations would be related to bedrock Hg concentrations as Richardson et al., (2018) showed argillite at Eel River CZO strongly influenced Hg inheritance. By estimating the inheritance or sequestration of atmospheric Hg, this study can highlight the importance of shale-driving Hg in soils and their potential release or capture from the terrestrial Hg biogeochemical cycle.

Materials and methods

Site descriptions

Seven sites were chosen from central New York to eastern Tennessee due to their similar lithology, ranging from Upper Devonian to Pennsylvanian shale, and span nearly 7° latitude. General lithology was evaluated using digital United States Geological Survey maps and tools to identify shale formations and groups (<https://mrdata.usgs.gov/geology/state/>). Satellite orthoimagery, USGS state geologic maps, and Google© street view were used to identify outcrops and road cuts to sample. To avoid artifacts from variations in the bedrock, organic-poor non-black shales were studied. When visiting each site, the sedimentary clast and organic composition of shale were verified and additional sites were rejected due to their variation in sand or silt and organic content. Moreover, areas with any surficial disturbances, e.g., logging roads, hiking trails, recent tree throw, were avoided. Mean annual temperature (MAT) and mean annual precipitation (MAP) for 30-year averages from 1980 to 2010 was obtained from the nearest weather station for each site (NOAA, 2011). All sites are forested,

with northern hardwoods transitioning into mixed hardwoods at more southern sites; the most dominant species were *Quercus* spp., *Carya* spp., *Acer* spp., *Fagus grandifolia*, *Juglans* spp., and *Populus* spp. with interspersed conifers, dominated by *Pinus* spp. and *Tsuga canadensis*.

Soil and bedrock sampling and processing

At each site, an upland location on shoulder slopes of hills and plateaus was identified. Soil pit locations were rejected if evidence of erosion, sediment deposition, microtopographical lows, or shallow groundwater was identified. At each site, one soil pit was excavated using stainless-steel tile spades until refusal for both shovels and pry bars. The lower boundary of the soil pits was characterized by chips of shale (shale fragments of 50 to 150 mm) indicating transition from soils to weathered shale. One kilogram samples were collected using a stainless-steel trowel for each 5-cm depth increment from the soil surface to the lower boundary of excavation. To accurately capture the geochemistry of the bedrock, at least three samples of unweathered shale and partially weathered highly were collected from either a road-cut exposure or a natural outcrop. Extent of weathering was determined in the field by visual and physical inspection for friability, cohesion, internal hydration, evidence of leaching or precipitation, and presence of oxidation.

Soils and weathered bedrock samples were spread thin onto aluminum tins and dried in a convection oven at 70 °C for 72 h. Oven-drying has been shown to be more effective in preventing the loss of gaseous Hg from soils by preventing microbial oxidation/reduction, diminishing Hg losses to < 3% (Hojdová et al., 2015). After drying, soils were sieved to < 2 mm, often using a stainless-steel hammer to disaggregate the clay-rich soil peds of the Bt horizons. Weathered and unweathered shale rock samples were ground with a tungstate mill and passed through a 100-mesh sieve (< 150 µm).

Soil pH was used to determined using a 2:5 soil—water slurry method. In brief, 4 g of soil and 10 g of 0.1 M CaCl₂, shaken, settled overnight and the pH of the supernatant extract, were measured with a VWR 8051 pH meter. Loss on ignition was used to estimate % soil organic matter (SOM) and measured by combusting a 5-g oven-dried subsample at 550 °C for 8 h. Every 20 samples included one blank and

duplicate. Samples were analyzed for soil particle size distribution using sedimentation columns and Bouyoucos hydrometer method (Gee & Bauder, 1986). For each analysis, ~ 30 g of dried soil was weighed into 250-mL glass beaker. Organic matter was removed and added 100 mL of 1 M sodium hexametaphosphate (HMP) solution to the soil for at least 8 h to disperse soil particles. This HMP-soil slurry was washed out into a 1000-mL graduated cylinder with DI water. A modified Bouyoucos hydrometer method was used, with hydrometer readings at 60 s and 1.5 h after mixing to the closest 0.5 g L^{-1} .

Total element quantification

Total Hg concentrations for regolith subsamples were quantified using a direct mercury analyzer-80 (Milestone Inc.). For the Hg measurement, 100 ± 10 mg of finely ground and homogenized subsamples was weighed into steel boats and ashed at $650 \text{ }^\circ\text{C}$, trapping Hg on gold amalgam. The gold amalgam is heated to $850 \text{ }^\circ\text{C}$, and Hg is quantified by an atomic absorption spectrophotometer. To ensure quality, every 15 samples included a duplicate, a preparation blank and SRM. NIST San Joaquin Soil 2709a was used as a standard reference material (SRM) (National Institute of Standards and Technology, Gaithersburg, MD). Preparation blanks were below detection limits ($< 0.05 \text{ ng/g}$), and duplicate variations were within 5%. SRM Hg measurements were within 10% of their certified values, with recovery rates for SRM NIST 2709a being 92% to 103%.

Subsamples of soils and rocks were analyzed for elemental constituents by total digestion. First, a 50-mg subsample digestion was placed in a 15-mL PFLA vial with 2.5 mL of 25 M HF acid and 2.5 mL of distilled 16 M HNO_3 (trace metal grade, VWR Analytical, Radnor, PA, USA), sealed with a lid and heated to $150 \text{ }^\circ\text{C}$. After complete digestion of most visible materials, samples were dried to volatilize Si-F complexes and redissolved in 5 mL of 8 M HNO_3 and re-sealed and heated to $150 \text{ }^\circ\text{C}$. The final digestate was diluted to 50 mL using 18.2 M Ω deionized water. With every 20 samples, at least one preparation blank, one duplicate, and a standard reference material (SRM) USGS SBC-1 were included.

Sequential extraction of oxidizable and reducible Hg fractions

A sequential extraction was performed to quantify the phase partitioning of Hg in soils and bedrock (see Issaro et al., 2009 for a review on methodological comparisons). The first extraction was to oxidize organic matter and reduced phases. First, a 1 g of soil or bedrock was extracted by slowly adding 20 mL of 15% H_2O_2 solution over 4 h and then shaking for 20 h. The slurry was centrifuged at 3000 rpm for 1 h, and the supernatant was transferred to a 50-mL centrifuge tube. The remaining extractant was reduced to extract secondary Fe oxide phases using a modified citrate-bicarbonate-dithionite extraction (Mehra & Jackson, 2013). In brief, 0.5 g of sodium dithionite was added to the remaining soil mass. Then, 40 mL of 0.1 M sodium citrate buffered with 0.1 M sodium bicarbonate solution was added to each tube and sealed tightly. The extracts were then heated to $60 \text{ }^\circ\text{C}$ in a convection oven for 12 h. For elemental analysis, both the oxidizable and reducible fractions were diluted with 5 g oxidizable extract diluted with 5 g of 2.5% HNO_3 solution and 0.2 g of the reducible fraction diluted with 14.8 g of 2.5% HNO_3 solution. Since the reducible fraction was under basic conditions at pH 8.1 and utilized high-sodium concentrations, it was imperative to use a small amount to keep metals and citrate in solution while acidifying. Extracts were analyzed for Hg with an Agilent 7700 \times Inductively Coupled Plasma-Mass Spectrometry (ICP-MS). With every 20 samples, a preparation blank, a duplicate, and a NIST San Joaquin 2709a were included. The CVs for the oxidizable fraction and reducible fraction of the NIST San Joaquin 2709a were 12% and 14%, respectively, and procedural blanks of Hg were 0.8 ng/g.

Instrumental analyses

Total digests and oxidizable and reducible extracts were analyzed for Fe and other macroelements using an Agilent 5110 Inductively Coupled Plasma-Optical Emission Spectrometer (Agilent Technologies, Santa Clara, California, USA). Iron concentrations in the preparation blank were $< 0.01 \text{ mg/kg}$, and all duplicates were within 15% CV. Iron recovery in the total digestions for USGS SBC-1 was 92% of their certified values. Since oxidizable and reducible fraction are not

certified methods, oxidizable Fe (Fe_{OX}) and reducible Fe (Fe_{RED}) cannot be certified for precision and accuracy. Mercury concentrations in the oxidizable and reducible fractions and total Ti were analyzed with an Agilent 7700 × Inductively Coupled Plasma-Mass Spectrometer. Mercury in the preparation blank was below the limit of quantification, and all duplicates were within 18% CV, Ti concentrations were < 0.1 ng/g in the preparation blanks and duplicates were with 15% CV. Recovery for Ti in USGS SBC-1 by total digestion was 84% of its certified values. Since oxidizable and reducible fraction are not certified methods, oxidizable Hg (Hg_{OX}) and reducible Fe (Hg_{RED}) cannot be certified for precision and accuracy.

Quantifying inherited and added Hg and other data analyses

Mass transfer coefficients (τ) of Hg were calculated to measure the degree of depletion or enrichment of regolith, relative to the parent material, for specific elements using Ti as an index element (Brantley & Lebedeva, 2011; Brimhall & Dietrich, 1987) and Eq. 1 is derived from Anderson et al., (2002). Mass transfer coefficients are defined for the element of interest (Mn and Fe) (j) in the weathered soil or regolith sample (w) normalized to an immobile index element Ti (i) in the parent material (p).

$$\tau_{j,w} = \frac{C_{j,w}C_{i,p}}{C_{j,p}C_{i,w}} - 1 \quad (1)$$

The variables $C_{j,w}$ and $C_{i,w}$ are equal to total concentrations of the element of interest (Mn and Fe) and Ti in the weathered samples, respectively, and $C_{j,p}$ and $C_{i,p}$ are the element of interest and Ti concentrations in the parent material (here, the least weathered regolith material) (e.g., Brimhall & Dietrich, 1987; Anderson, 2002). Negative τ values indicate a net loss of an element from a specific depth due to leaching. Positive τ values indicate a net enrichment of an element.

Mercury was referenced to Ti in the deepest weathered bedrock samples in each regolith profile (Grimaldi et al., 2008; Guedron et al., 2006; Zhang et al., 2015). Titanium exists in higher concentrations and avoids errors associated with anomalies in zircon crystal abundance and incomplete zircon digestion.

This method assumes that the element Ti contained in the parental material undergoes similar pedogenic processes as Hg within the soil sourced from weathering of the shale bedrock, with the caveat that Ti will remain, while Hg can leach away or be added from atmospheric deposition to the soil profile.

The association of Hg, Hg_{OX}, and Hg_{RED} with Fe_{RED}, as an estimate for secondary Fe oxides, soil pH, and %LOI as a proxy for organic matter, was tested using linear regressions across all sites using MATLAB (Matlab 2016, Mathworks, Natick, MA). In addition, total soil profile and surface soil (0–30 cm) Hg and soil properties were compared with MAT and MAP for each site using linear regressions (Table 2).

Results

Mercury concentration across the climate gradient

For the first hypothesis, Hg profiles for the seven weathering profiles were investigated, from surface soils to unweathered shale to determine whether greater organic matter or Fe oxides promote Hg retention. All soils were clay-rich Ultisols or Alfisols (Table 1). Soil total Hg concentrations at Sites 1 through Site 7 ranged from a low of 18 ng/g for 68 cm at Site 3 to a high of 265 ng/g for 12.5-cm depth at Site 2 (Fig. 2; Supplemental Table 1). Total Hg concentrations were greatest in the surface soils in the top 20 cm for Site 2 and Site 3 (Fig. 2). Total Hg concentrations decreased with depth and were lowest in the shale bedrock for weathering profiles at all Sites except Site 1, where bedrock concentrations (94 ng/g) were higher than all other soil horizons (57–80 ng/g). Further, unweathered and weathered shales at Site 1 had significantly higher total Hg concentrations than shales at all other sites (Supplemental Table 1, Fig. 2).

Similar to total Hg concentrations, Hg_{OX} were greatest in the surface soils in the top 20 cm for Site 2 and Site 3 (Fig. 2) and ranged from 2 to 216 ng/g across all sites and rocks and soils. Hg_{OX} decreased with depth and was lowest in the shale bedrock for weathering profiles at all Sites except Site 1, where bedrock Hg_{OX} concentrations (38 ng/g) were comparable to other soil horizons (19–59 ng/g). Unweathered and weathered shale at Site 1 had higher Hg_{OX} concentrations (38 ng/g) than shales at all other sites

Fig. 1 Map of study locations with satellite imagery by ESRI generated using ArcGIS 10.8.1 © ESRI

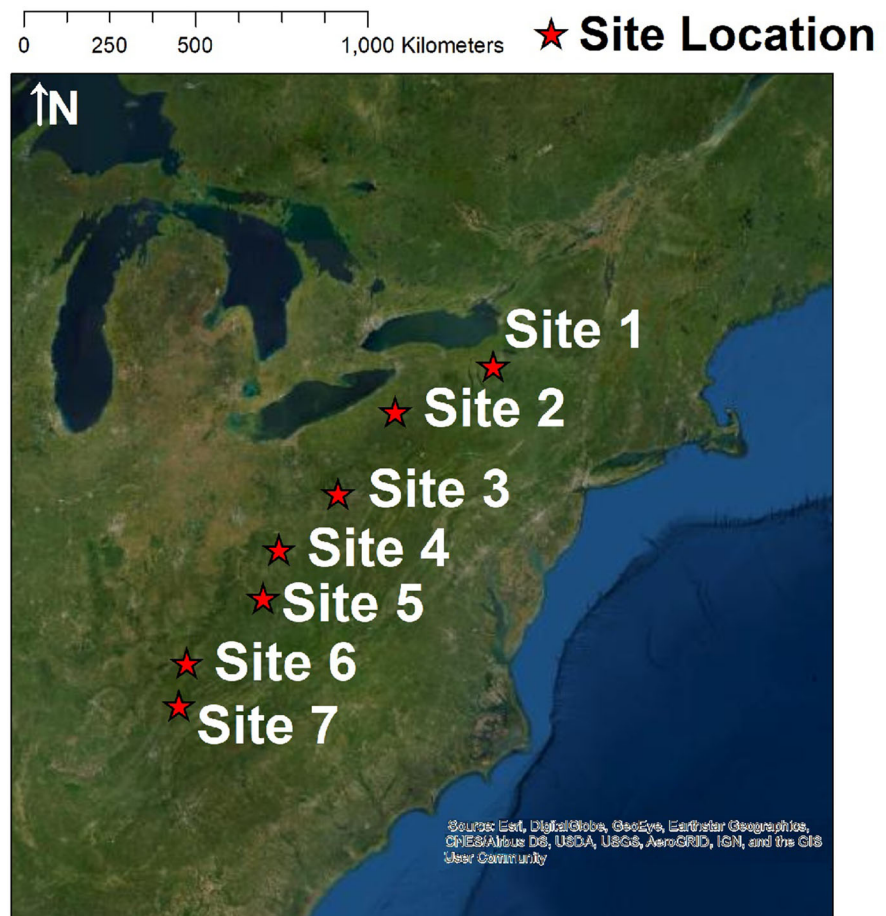


Table 1 Site locations, lithology, and soil taxonomy and setting. Climate data were obtained from NOAA

Site #	Site code	Longitude	Latitude	MAT °C/yr	MAP mm/yr	Soil series	Great group	Age/Rock	Landform
Site 1	MAR	- 76.325747	42.90819	8.6	1067	Schoharie silty clay	Hapludalfs	Middle Devonian Shale	Hill and hillslope
Site 2	ANF	- 78.889138	42.0367	7.3	1135	Rayne silt loam	Hapludults	Upper Devonian Shale	Hills, Plateaus
Site 3	RCSP	- 80.386657	40.42054	11.1	960	Dormont silt loam	Hapludalfs	Pennsylvanian Shale	Hill and hillslope
Site 4	WCHT	- 81.938559	39.30305	11.0	1001	Westmoreland silt loam	Ultic Hapludalfs	Pennsylvanian Shale, Siltstone, Mudstone	Hill and hillslope
Site 5	BFSP	- 82.348515	38.30369	12.3	1138	Gilpin-Upshur silt loam	Hapludults	Pennsylvanian Shale, Siltstone, Mudstone	Ridge, hill, and hillslope
Site 6	DBNF	- 84.345846	36.95657	13.2	1255	Shelocta-Rigley-Latham-Lily	Hapludults	Pennsylvanian Shale, Siltstone	upland areas, foot slopes
Site 7	LMSP	- 84.552052	36.07218	14.9	1293	Lonewood silt loam	Hapludults	Pennsylvanian Shale, Sandstone	Rolling plateaus

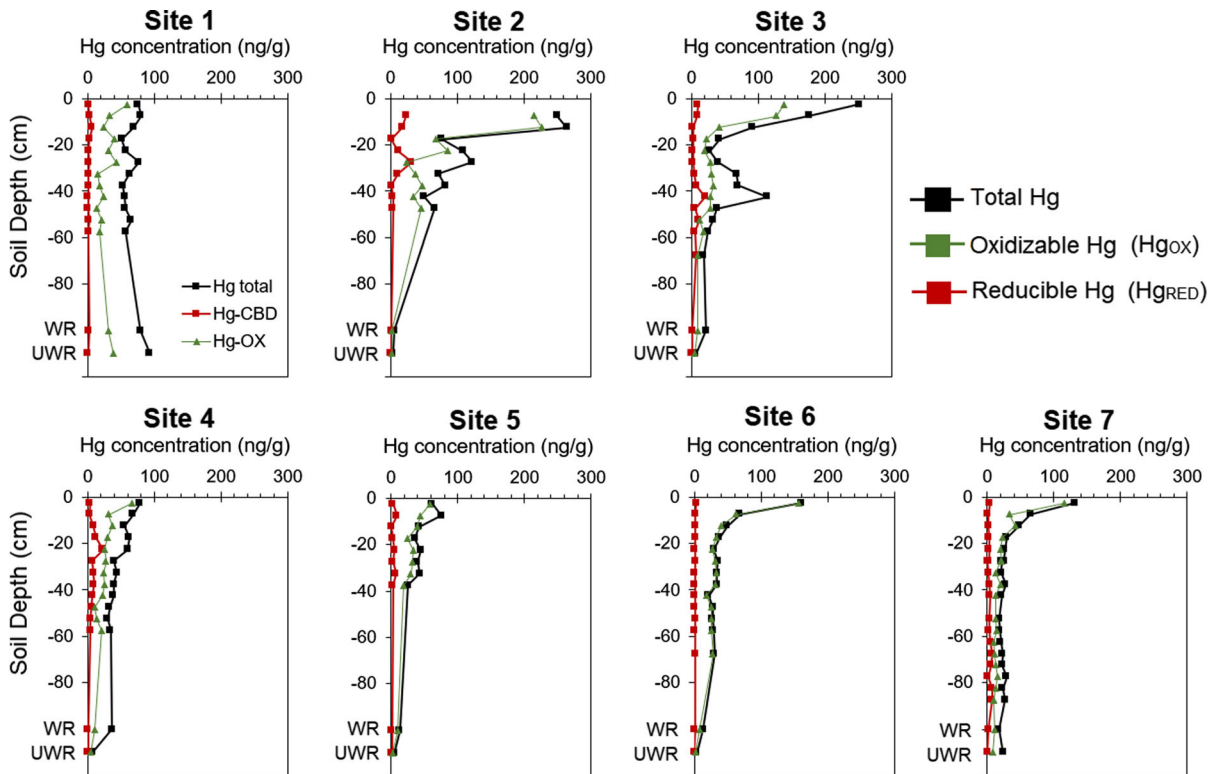


Fig. 2 Total Hg concentrations, reducible Hg fraction, and oxidizable Hg fractions for soil profiles and rock samples (weathered, unweathered) for each site

(ranging 1.7 to 7.6 ng/g). Across soils and rocks from all sites, Hg_{OX} comprised a large portion of the total Hg at $63\% \pm 8\%$ on average.

Across all sites, Hg_{RED} concentrations were lower than Hg_{OX} in all soil horizons and in weathered and unweathered shale samples, ranging from 0.6 to 32 ng/g. Hg_{RED} did not exhibit a pattern with depth in the soil profile, but Hg_{RED} concentrations were lowest in the shale bedrock for weathering profiles at all Sites (0.6–1.6 ng/g). Unweathered and weathered shale Hg_{RED} concentrations did not differ among sites (ranging 0.6 to 1.6 ng/g). Across rocks and soils at all sites, Hg_{RED} comprised only a small fraction of $10\% \pm 4\%$ of the total Hg on average.

%LOI and soil pH exhibited differences among sites and with depth (see Supplemental Fig. 1). Soil pH was much higher at Site 4 and Site 5 (5.5–6.7) but lower at Site 2 (3.1–4.2). Soil pH was typically lower in the surface soils of 0–10 cm depths but similar with from 20 or 30 cm depth to the bottom of the profile. Soil %LOI was greatest in surface soils in the 0–15 cm in depths (7%–50% LOI), which coincide with the

lowest soil pH values. %LOI was greatest in surface soils at Site 2. Soil texture was generally comparable for most sites: Sites 1, 4, 5, 6, were loams, Sites 2 and 6 were silt loams, Site 7 was a clay loam and clay contents ranged from 11 to 35% across the seven sites. Linear regressions were utilized to explore basic causal relationships in total Hg, Hg_{OX}, and Hg_{RED} with soil properties (Table 2). %LOI was strongly correlated with total Hg ($R = 0.65$) and Hg_{OX} ($R = 0.76$) but poorly correlated with Hg_{RED} ($R = 0.39$). Soil pH was poorly correlated with total Hg ($R = -0.23$) and Hg_{OX} ($R = -0.30$) and Hg_{RED} ($R = 0.09$). Soil Fe_{RED} was poorly correlated with total Hg ($R = 0.10$) and Hg_{OX} ($R = -0.13$) and Hg_{RED} ($R = 0.29$). Clay content of the soil was poorly correlated with total Hg ($R = 0.13$) and Hg_{OX} ($R = 0.17$) and Hg_{RED} ($R = 0.19$).

Further, the relationship between climate and median soil profile Hg concentrations and soil properties was explored with linear regressions (Table 2). MAT was negatively correlated with the average soil

Table 2 Linear regression R coefficients for soil Hg (total Hg, oxidizable Hg, reducible Hg, and Hg tau (τ) values) and soil properties (pH, LOI, %clay), for entire profiles and climate

properties (mean annual temperature and mean annual precipitation) with median site values

	Fe _{RED}	pH	LOI	%Clay				
Hg Total	- 0.10	- 0.23	0.65	0.19				
Hg _{OX}	- 0.13	- 0.30	0.76	0.22				
Hg _{RED}	0.29	0.09	0.45	0.17				
	Fe _{RED}	pH	LOI	%Clay	Hg Total	Hg _{OX}	Hg _{RED}	Hg τ
MAT	0.27	- 0.07	- 0.52	- 0.11	- 0.92	- 0.67	- 0.46	- 0.64
MAP	0.33	- 0.54	- 0.16	0.08	- 0.30	- 0.03	- 0.52	- 0.03

Bold text indicates a regression is significant at $p < 0.05$

profile total Hg, Hg_{RED}, and Hg_{OX} concentrations ($R = - 0.84, - 0.55, - 0.63$, respectively), %LOI ($R = - 0.52$), and Hg τ values ($R = - 0.64$). MAT was not correlated with the average soil profile Fe_{RED}, pH, or clay content. MAP was negatively correlated with total soil profile Hg_{RED} concentrations ($R = - 0.50$) and pH ($R = - 0.54$). MAP was not correlated with the average soil profile Fe_{RED}, pH, or clay content, total Hg concentrations, Hg_{OX} concentrations, or Hg τ values (Table 2).

Hg losses and additions

In the second hypothesis, τ for total Hg concentrations indexed to Ti was investigated to determine the extent

of Hg losses and additions from bedrock inheritance or atmospheric inputs. All sites exhibited net sequestration of added Hg (Fig. 3) except for Site 1, which showed very little Hg enrichment but showed some depletion (τ values $- 0.4$ to 0.3 ; Fig. 3). Site 7 shows high Hg enrichment in the top 20 cm (τ values 2.5 to 10.6) but decreasing enrichment in subsurface horizons (τ values $- 0.5$ to 1.1). Sites 3, 4, 5, and 6 showed high levels of Hg enrichment throughout their soil profiles (τ values 3.1 to 40). However, site 2 showed substantially high levels of Hg enrichment from 0 to 40 cm depth (τ values 25 to 321). Contrary to the hypothesis, the variations in τ values did not correspond with site climatic data, as surface (0–10 cm) and subsurface (30 to 50 cm) τ values were poorly correlated with MAT and MAP for the seven sites.

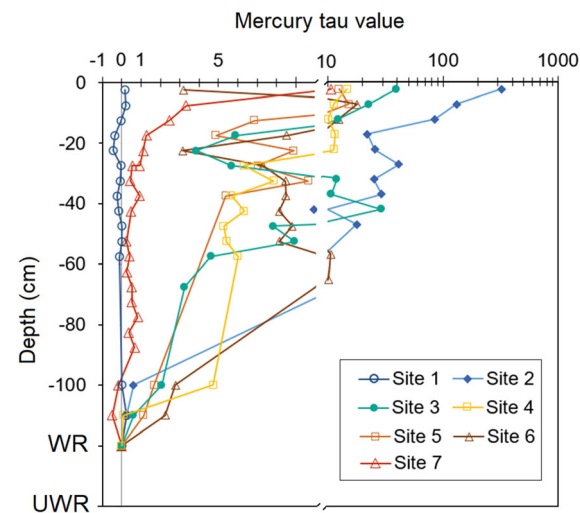


Fig. 3 Total Hg tau values for each soil horizon and weathered rock (WR) using the unweathered rock (UWR) samples at each site as the parent material and Ti as the reference element

Discussion

Mercury concentrations in weathering profiles across the climate gradient

For the first hypothesis, it was expected that Hg concentrations in soils would differ with climate, particularly that extended pedogenesis in warmer, wetter sites would generate greater secondary Fe oxide abundance or less organic matter for Hg sorption. From the linear regressions, warmer and wetter sites did not have significantly higher secondary Fe oxide abundance in soil profiles but did have less organic matter. Further, it was observed that sites with less organic matter also had lower soil profile Hg_{OX} and

total Hg concentrations and that 68% of total Hg on average was in the Hg_{OX} phase. These results show that instead of extent of soil development, soils with more organic matter had accumulated or retained more Hg and that organic matter bound Hg represented the largest fraction of Hg in soils. Conversely, warmer sites did not have more Fe oxides and Hg_{RED} was < 20% of the total Hg for nearly all soil horizons across the seven sites. Thus, the data suggest that organic matter played an important role in Hg accumulation across the climatic gradient rather than Fe oxides. Moreover, the soils in warmer climates (Sites 6 and 7) had less subsurface organic matter and lower Hg concentrations (Fig. 2; Supplemental Fig. 1). This agrees with previous studies that found organic matter as the principal factor controlling Hg accumulation in soil (e.g., Obrist et al., 2009; Obrist et al., 2011; Richardson et al., 2013; Skyllberg et al., 2000; Xue et al., 2019; Yu et al., 2014). Site 1 was anomalous, as it had the lowest organic matter content but higher total Hg concentrations throughout the soil profile. Moreover, only about half of the Hg was associated with an organic phase and very little associated with Fe oxide phase. Thus, another important phase, likely inherited from the shale bedrock, must be present at Site 1, which is further discussed in “[Sequestration of atmospheric Hg](#)” section. Overall, these results highlight the importance of organic matter for sequestration of Hg.

There are some important details to note on the relationship between Fe_{RED} and soil Hg concentrations. Secondary Fe oxides had only < 20% of the total Hg, but their effect on soil Hg may not have been as pronounced as observed in extensively studied tropical soils (e.g., Fiorentino et al., 2011; Grimaldi et al., 2008; Roulet et al., 1998). The variation in Fe oxides may not have been extensive enough to fully capture their effect. The freeze-thaw cycles and saturated conditions during transitions between winter and summer seasons may limit precipitation of secondary Fe oxides and shift toward physical weathering. Further, Sites 1 and 2 are within the glacial and periglacial extent of the last glacial maximum 22 kya, respectively. Thus, Site 1 soils are the youngest and Site 2 soils are younger and less developed and lack the pedogenesis to develop deep secondary Fe oxide formations. Another caveat is that the Hg_{OX} phase is a non-specific phase that aims for the oxidation of organic and organo-mineral complexes (Issaro et al.,

2009). The oxidation of soil could also solubilize HgS present in the soils and shales (see Biester et al., 2000; Richardson et al., 2018), but the effect remains unknown as HgS was not quantified in this study. Despite these caveats, the results show that Hg sequestration is occurring predominantly through complexation with organic matter as opposed to Fe oxides.

Sequestration of atmospheric Hg

In the second hypothesis, the provenance of Hg was explored by comparing Hg concentration weathering profiles from surface soils to unweathered shales and using τ values normalizing Hg to Ti. It was expected that soils derived from shales with higher Hg concentrations would inherit Hg and also have high Hg concentrations. However, the weathering profiles show that Hg concentrations decreased with depth and had their lowest Hg concentrations in unweathered shales, except for Site 1. For all sites except Site 1, Hg τ values suggest that Hg was not depleted from shale-derived soils, but was being added from the atmosphere and sequestered in shale-derived soils (e.g., Richardson & Friedland, 2015; Richardson et al., 2018; Yu et al., 2014). Moreover, unweathered shale concentrations were comparable across sites, except Site 1, which had the highest Hg concentrations but the lowest Hg τ values. This also suggests that sequestration of Hg in shale-derived soils was not controlled by inherited Hg concentrations, except for Site 1. Site 1 was different from the other sites with moderate Hg concentrations and Hg τ values centering around zero with depth. It is hypothesized that the homogeneity with depth and limited enrichment or depletion was due to being very young from the most recent glaciation.

The results demonstrate that Hg accumulation in shale-derived soils was affected by climate, with cooler, organic matter-rich soils sequestering more Hg concentrations than warmer, less organic-rich soils. MAT was negatively correlated to Hg τ values, and the coldest site, Site 2, had the greatest enrichment of Hg in the soil profile and the warmest site, Site 7, had the second lowest enrichment of Hg in the soil profile (Fig. 3). These findings suggest climate may be important for Hg concentrations, particularly due to its role in organic matter retention. The link between organic matter and Hg is a well-established

observation (e.g. Obrist et al., 2011; Richardson et al., 2013; Sklyberg et al., 2000; Xue et al., 2019; Yu et al., 2014). Moreover, the findings suggest as soils and soil materials age, they accumulate Hg from the atmosphere and are less controlled by bedrock inherited Hg.

In addition to organic matter, proximity to pollution sites was also another driver of the variation Hg enrichment in the studied shale-derived soils. Total Hg concentrations at Sites 1, 4, 5, 6, and 7 were comparable to the range of values reported by previous studies on non-point-source-polluted forested soils in North America (e.g., Obrist et al., 2011; Richardson & Friedland, 2015; Richardson et al., 2013), temperate and subtropical China (Luo et al., 2014; Zhang et al., 2018), and temperate Europe (Schwesig & Matzner, 2001). However, Sites 2 and 3 had total Hg concentrations in surface soils comparable to those on the lower end of point-source-polluted areas such as soils near artisanal gold mining (e.g., 70–420 ng/g soils in French Guiana studied by Guedron et al., 2006), coal-fired power plant in Spain (1–7560 ng/g Martin & Nanos, 2016), and soils near metropolitan areas in China (e.g., 110–2178 ng/g in Shi et al., 2013; Zhang et al., 2018) and metropolitan areas in the northeastern USA (68 to 712 ng/g Richardson & Moore, 2020). Sites 2 and 3 had the highest surface soil Hg τ values and are located downwind of extensive use of past coal combustion power plants. For example, atmospheric deposition of Hg has been greater in southeastern Ohio compared with Pennsylvania and New York (Risch et al., 2012). The higher deposition of Hg in the region has been due to local and regional coal combustion sources in the Ohio River Valley, which Keeler et al (2006) was able to attribute $\sim 70\%$ of deposition was sourced from coal combustion. Thus, it may be concluded that while organic matter provided the sequestration and sorption capacity, human activities such as coal combustion could have led to the enrichment Hg in the surface soils above background rates (Streets et al., 2017, 2019).

There are a few assumptions that must be considered. Since the sampling locations were upland positions, it may be surmised that Hg was sourced from atmospheric deposition and lateral transport can be assumed to be negligible. Moreover, since upland positions on hill slopes, benches, and plateaus were sampled, it can be assumed that erosion has not impacted these soils and that soils at Sites 1–3 have been stable since the last glacial maximum and Sites

4–7 have been stable for > 20 kya. Black shales were not studied and could have a different effect on black shale-derived soils, in particular higher Hg concentrations, greater inherited organic matter, and higher Fe contents (Fu et al., 2015), all of which could affect sorption and retention. However, black shales are highly variable and were not studied for that reason. Another assumption and potential source of error with the Hg/Ti normalization are that Ti may be mobile in the surface soil (e.g. Buss et al., 2017), meaning that Hg/Ti could be overestimated and leading to cause an underestimation of Hg inherited from shale. It is assumed that the homogenization of finely ground soil samples avoided Ti mobilization bias.

Conclusions and implications for regional and global Hg biogeochemistry

Sequestration and not depletion of Hg from shales from New York to Tennessee have many implications for regional ecotoxicology and the global Hg biogeochemical cycle. First, this result demonstrates that shale-derived soils can retain Hg pollution and prevent its movement to local lakes and rivers, where fishing is a popular recreational activity. Second, unlike other sedimentary systems, the shale units studied did not appear to be an important source of Hg regolith. For example, substantial Hg concentrations and methyl-Hg pollution in the South Fork Eel River of California are geologically sourced (Tsui et al., 2014; Richardson et al., 2018). Lastly, the finding suggests that shale-derived soils do sequester Hg through stabilization by organic matter; however, if climate change increases decomposition rates of organic matter, then less Hg may be released sequestered.

Acknowledgements Justin Richardson would like to thank Sumaya Hamdi and Corey Palmer for excavating and collecting the samples as well as Mark Butler, Ainsley McStay, and Eliza Fitzgerald for partial soil sample preparations.

Author contributions Justin Richardson designed the study, processed, and analyzed the samples, completed the statistical analyses and interpretations, and wrote the entire manuscript.

Funding This project was funded by the University of Massachusetts Amherst College of Natural Sciences with a grant to Justin Richardson.

Data availability Mercury concentration data are available in Supplemental Information.

Code availability Software used to analyze the data is available in MATLAB version 2016 and Microsoft Excel 2010.

Declarations

Conflict of interest The author states there are no conflicts of interests.

Consent to participate No human subjects were used in this research.

Consent for publication No human subjects were used in this research.

Human and animal rights No animals were used in this research.

References

Adriano, D. C. (2001). *Mercury. In Trace elements in terrestrial environments*. Springer.

Amos, H. M., Jacob, D. J., Streets, D. G., & Sunderland, E. M. (2013). Legacy impacts of all-time anthropogenic emissions on the global mercury cycle. *Global Biogeochemical Cycles*, 27, 410–421.

Anderson, S. P., Dietrich, W. E., & Brimhall, G. H., Jr. (2002). Weathering profiles, mass-balance analysis, and rates of solute loss: Linkages between weathering and erosion in a small, steep catchment. *Geological Society of America Bulletin*, 114(9), 1143–1158.

Biester, H., Gosar, M., & Covelli, S. (2000). Mercury speciation in sediments affected by dumped mining residues in the drainage area of the Idrija mercury mine, Slovenia. *Environmental Science & Technology*, 34(16), 3330–3336.

Brantley, S. L., & Lebedeva, M. (2011). Learning to read the chemistry of regolith to understand the critical zone. *Annual Review of Earth and Planetary Sciences*, 39, 387–416.

Brimhall, G. H., & Dietrich, W. E. (1987). Constitutive mass balance relations between chemical composition, volume, density, porosity, and strain in metasomatic hydrochemical systems: Results on weathering and pedogenesis. *Geochimica Et Cosmochimica Acta*, 51, 567–587.

Buss, H. L., Lara, M. C., Moore, O. W., Kurtz, A. C., Schulz, M. S., & White, A. F. (2017). Lithological influences on contemporary and long-term regolith weathering at the Luquillo critical zone observatory. *Geochimica Et Cosmochimica Acta*, 196, 224–251.

Driscoll, C. T., Mason, R. P., Chan, H. M., Jacob, D. J., & Pirrone, N. (2013). Mercury as a global pollutant: Sources, pathways, and effects. *Environmental Science & Technology*, 47, 4967–4983.

Fiorentino, J. C., Enzweiler, J., & Angélica, R. S. (2011). Geochemistry of mercury along a soil profile compared to other elements and to the parental rock: Evidence of external input. *Water, Air, & Soil Pollution*, 221, 63–75.

Fu, X., Wang, J., Tan, F., Feng, X., Zeng, S., Chen, W., & Wang, D. (2015). Minerals and potentially hazardous trace

elements in marine oil shale: New insights from the Shengli River North surface mine, northern Tibet, China. *Environmental Earth Sciences*, 73(7), 3137–3157.

Gabriel, M. C., & Williamson, D. G. (2004). Principal biogeochemical factors affecting the speciation and transport of mercury through the terrestrial environment. *Environmental Geochemistry and Health*, 26, 421–434.

Gee, G. W., Bauder, J. W., & Klute, A. (1986). *Methods of soil analysis, part 1, physical and mineralogical methods*. Soil Science Society of America.

Grimaldi, C., Grimaldi, M., & Guedron, S. (2008). Mercury distribution in tropical soil profiles related to origin of mercury and soil processes. *Science of the Total Environment*, 401, 121–129.

Guedron, S., Grimaldi, C., Chauvel, C., Spadini, L., & Grimaldi, M. (2006). Weathering versus atmospheric contributions to mercury concentrations in French Guiana soils. *Applied Geochemistry*, 21, 2010–2022.

Hojdová, M., Rohovec, J., Chrástný, V., Penížek, V., & Navrátil, T. (2015). The influence of sample drying procedures on mercury concentrations analyzed in soils. *Bulletin of Environmental Contamination and Toxicology*, 94, 570–576.

Holmes, P., James, K. A. F., & Levy, L. S. (2009). Is low-level environmental mercury exposure of concern to human health? *Science of the Total Environment*, 408, 171–182.

Hosterman, J.W. and Whitlow, S.T., 1981. Clay mineralogy of Devonian shales in the Appalachian Basin. Geol. Surv. Open-File Rep. (US);(United States), 81.

Hylander, L. D., & Meili, M. (2003). 500 years of mercury production: Global annual inventory by region until 2000 and associated emissions. *Science of the Total Environment*, 304, 13–27.

Issaro, N., Abi-Ghanem, C., & Bermond, A. (2009). Fractionation studies of mercury in soils and sediments: A review of the chemical reagents used for mercury extraction. *Analytica Chimica Acta*, 631(1), 1–12.

Keeler, G. J., Landis, M. S., Norris, G. A., Christianson, E. M., & Dvonch, J. T. (2006). Sources of mercury wet deposition in eastern Ohio, USA. *Environmental Science & Technology*, 40, 5874–5881.

Lamborg, C. H., Fitzgerald, W. F., O’Donnell, J., & Torgersen, T. (2002). A non-steady-state compartmental model of global-scale mercury biogeochemistry with interhemispheric atmospheric gradients. *Geochimica Et Cosmochimica Acta*, 66, 1105–1118.

Luo, Y., Duan, L., Wang, L., Xu, G., Wang, S., & Hao, J. (2014). Mercury concentrations in forest soils and stream waters in northeast and south China. *Science of the Total Environment*, 496, 714–720.

Martín, J. A. R., & Nanos, N. (2016). Soil as an archive of coal-fired power plant mercury deposition. *Journal of Hazardous Materials*, 308, 131–138.

Mehra, O. P., & Jackson, M. L. (2013). *Iron oxide removal from soils and clays by a dithionite–citrate system buffered with sodium bicarbonate. In Clays and clay minerals* (pp. 317–327). Cham: Pergamon.

National Oceanographic and Atmospheric Administration (NOAA) (2011) Climate Data Online: Monthly Observational Data. U.S. Department of Commerce, National Oceanic and Atmospheric Administration, National

- Environmental Satellite Data and Information Service, National Climatic Data Center. <http://www.ncdc.noaa.gov/cdo-web/>.
- Nriagu, J., & Becker, C. (2003). Volcanic emissions of mercury to the atmosphere: Global and regional inventories. *Science of the Total Environment*, *304*, 3–12.
- Obrist, D., Johnson, D. W., & Lindberg, S. E. (2009). Mercury concentrations and pools in four Sierra Nevada forest sites, and relationships to organic carbon and nitrogen. *Biogeochemistry*, *6*, 765–777.
- Obrist, D., Johnson, D. W., Lindberg, S. E., Luo, Y., Hararuk, O., Bracho, R., Battles, J. J., Dail, D. B., Edmons, R. L., Monson, R. K., Ollinger, S. V., Pallardy, S. G., Pregitzer, K. S., & Todd, D. E. (2011). Mercury distribution across 14 U.S. forests. Part 1: Spatial patterns of concentrations in biomass, litter, and soils. *Environmental Science and Technology*, *45*, 3974–3981.
- Richardson, J. B., & Friedland, A. J. (2015). Mercury in coniferous and deciduous upland forests in northern New England, USA: Implications of climate change. *Biogeochemistry*, *12*, 6737–6749.
- Richardson, J. B., & Moore, L. (2020). A tale of three cities: Mercury in urban deciduous foliage and soils across landuses in Poughkeepsie NY, Hartford CT, and Springfield MA USA. *Science of The Total Environment*, *715*, 136869.
- Richardson, J. B., Friedland, A. J., Engerbretson, T. R., Kaste, J. M., & Jackson, B. P. (2013). Spatial and vertical distribution of mercury in upland forest soils across the northeastern United States. *Environmental Pollution*, *182*, 127–134.
- Richardson, J. B., Aguirre, A. A., Buss, H. L., Toby O’Geen, A., Gu, X., Rempé, D. M., & Richter, D. D. B. (2018). Mercury sourcing and sequestration in weathering profiles at six critical zone observatories. *Global Biogeochemical Cycles*, *32*(10), 1542–1555.
- Risch, M. R., Gay, D. A., Fowler, K. K., Keeler, G. J., Backus, S. M., Blanchard, P., Barres, J. A., & Dvonch, J. T. (2012). Spatial patterns and temporal trends in mercury concentrations, precipitation depths, and mercury wet deposition in the North American Great Lakes region, 2002–2008. *Environmental Pollution*, *161*, 261–271.
- Roulet, M., Lucotte, M., Saint-Aubin, A., Tran, S., Rheault, I., Farella, N., Dezencourt, J., Passos, C. J. S., Soares, G. S., Guimaraes, J. R., & Mergler, D. (1998). The geochemistry of mercury in central Amazonian soils developed on the Alter-do-Chao formation of the lower Tapajos River Valley, Para state, Brazil. *Science of the Total Environment*, *223*, 1–24.
- Schuster, P. F., Schaefer, K. M., Aiken, G. R., Antweiler, R. C., Dewild, J. F., Gryziec, J. D., Gusmeroli, A., Hugelius, G., Jafarov, E., Krabbenhoft, D. P., & Liu, L. (2018). Permafrost stores a globally significant amount of mercury. *Geophysical Research Letters*, *45*, 1463–1471.
- Schwesig, D., & Matzner, E. (2001). Dynamics of mercury and methylmercury in forest floor and runoff of a forested watershed in Central Europe. *Biogeochemistry*, *53*, 181–200.
- Shi, J. B., Meng, M., Shao, J. J., Zhang, K. G., Zhang, Q. H., & Jiang, G. B. (2013). Spatial distribution of mercury in topsoil from five regions of China. *Environmental Science and Pollution Research*, *20*, 1756–1761.
- Skyllberg, U., Xia, K., Bloom, P. R., Nater, E. A., & Bleam, W. F. (2000). Binding of mercury (II) to reduced sulfur in soil organic matter along upland-peat soil transects. *Journal of Environmental Quality*, *29*(3), 855–865.
- Streets, D. G., Horowitz, H. M., Jacob, D. J., Lu, Z., Levin, L., Ter Schure, A. F., & Sunderland, E. M. (2017). Total mercury released to the environment by human activities. *Environmental Science & Technology*, *51*, 5969–5977.
- Streets, D. G., Horowitz, H. M., Lu, Z., Levin, L., Thackray, C. P., & Sunderland, E. M. (2019). Global and regional trends in mercury emissions and concentrations, 2010–2015. *Atmospheric Environment*, *201*, 417–427.
- Tsui, M. T. K., Blum, J. D., Finlay, J. C., Balogh, S. J., Nollet, Y. H., Palen, W. J., & Power, M. E. (2014). Variation in terrestrial and aquatic sources of methylmercury in stream predators as revealed by stable mercury isotopes. *Environmental Science & Technology*, *48*, 10128–10135.
- United States Energy Information Administration and Kuuskraa, V. 2011. World shale gas resources: an initial assessment of 14 regions outside the United States. US Department of Energy
- Vaughan, W. J., & Russell, C. S. (2015). *Freshwater recreational fishing: The national benefits of water pollution control*. Routledge.
- Xue, W., Kwon, S. Y., Grasby, S. E., Sunderland, E. M., Pan, X., Sun, R., Zhou, T., Yan, H., & Yin, R. (2019). Anthropogenic influences on mercury in Chinese soil and sediment revealed by relationships with total organic carbon. *Environmental Pollution*, *255*, 113186.
- Yu, X., Driscoll, C. T., Warby, R. A., Montesdeoca, M., & Johnson, C. E. (2014). Soil mercury and its response to atmospheric mercury deposition across the northeastern United States. *Ecological Applications*, *24*, 812–822.
- Zahir, F., Rizwi, S. J., Haq, S. K., & Khan, R. H. (2005). Low dose mercury toxicity and human health. *Environmental Toxicology and Pharmacology*, *20*, 351–360.
- Zhang, H., Li, Y., Luo, Y., & Christie, P. (2015). Anthropogenic mercury sequestration in different soil types on the southeast coast of China. *Journal of Soils and Sediments*, *15*(4), 962–971.
- Zhang, Y., Wang, M., Huang, B., Akhtar, M. S., Hu, W., & Xie, E. (2018). Soil mercury accumulation, spatial distribution and its source identification in an industrial area of the Yangtze Delta, China. *Ecotoxicology and Environmental Safety*, *163*, 230–237.

Publisher’s Note Springer Nature remains neutral with regard to jurisdictional claims in published maps and institutional affiliations.